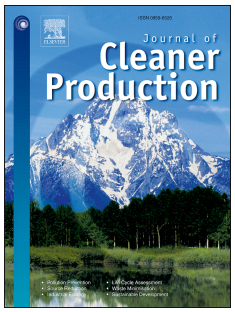

Quantifying influences of anthropogenic-natural factors on ecological land evolution in mega-urban agglomeration: A case study of Guangdong-Hong Kong-Macao Greater Bay Area

Rundong Feng, Fuyuan Wang, Kaiyong Wang, Shaojie Xu

PII: S0959-6526(20)35349-X

DOI: https://doi.org/10.1016/j.jclepro.2020.125304

Reference: JCLP 125304

To appear in: *Journal of Cleaner Production*

Received Date: 1 August 2020

Revised Date: 31 October 2020

Accepted Date: 27 November 2020

Please cite this article as: Feng R, Wang F, Wang K, Xu S, Quantifying influences of anthropogenic-natural factors on ecological land evolution in mega-urban agglomeration: A case study of Guangdong-Hong Kong-Macao Greater Bay Area, *Journal of Cleaner Production*, https://doi.org/10.1016/j.jclepro.2020.125304.

Author Contribution Statement

Rundong Feng: Conceptualization, Methodology, Software, Formal analysis, Writing- Original draft preparation.

Fuyuan Wang: Project administration, Research design, Supervision, Editing

Kaiyong Wang: Writing- Reviewing, Validation, Supervision

Shaojie Xu: Data curation, Formal analysis

Quantifying influences of anthropogenic-natural factors on ecological land evolution in mega-urban agglomeration: A case study of Guangdong-Hong Kong-Macao Greater Bay Area

Rundong Feng[a,b], Fuyuan Wang[a], Kaiyong Wang[a], Shaojie Xu[a,b]

[a] Institute of Geographic Sciences and Natural Resources Research, Key Laboratory of Regional Sustainable Development Modeling, Chinese Academy of Sciences, Beijing, 100101, China

[b] College of Resources and Environment, University of Chinese Academy of Sciences, Beijing, 100049, China

Rundong Feng: fengrd.18s@igsnrr.ac.cn

Fuyuan Wang (Corresponding author): wangfy.15b@igsnrr.ac.cn

Kaiyong Wang: wangky@igsnrr.ac.cn

Shaojie Xu: xusj.19s@igsnrr.ac.cn

Abstract: Modeling ecological land evolution and determining the responsible driving forces is a common research topic in land use and landscape ecology. However, the interaction effect and dynamic change of anthropogenic-natural factors on the ecological land evolution of urban agglomerations is still unclear. Supported by Google Earth Engine, this study used Landsat satellite imagery and random forest algorithm to obtain the land cover datasets of Guangdong-Hong Kong-Macao Greater Bay Area from 1990-2019. Furthermore, a geographic detector was used to identify the driving factors' impact on ecological land evolution by quantifying nonlinear associations, change characteristics, and mechanisms. The results show: (1) Ecological land shifted from decline and fragmentation (1990-2010) to growth and integration (2010-2019). (2) Population density (q=0.83) and land urbanization rate (q=0.75) mainly controlled the ecological land evolution, illustrating more explanatory power than other factors, and accounting for higher proportion of area as the determinant factor in the study region. All driving factors interactions were bivariate, and the interaction between population density and elevation had the largest influence (q=0.92). (3) Anthropogenic factors had a generally greater influence on ecological land than natural factors, and the impact of population density and GDP per capita exhibited a continuous increase, while land urbanization rate first decreased (1990-2000) and then increased (2000-2019) in response to industrial restructuring and accelerated urbanization. Due to the intensification of anthropogenic activities, the effect of average annual temperature and precipitation declined by 69% and 77%, respectively. The conclusions indicate that the interaction and spatially heterogeneous

distribution of anthropogenic-natural factors should be comprehensively considered when designing a system based on cooperative mechanisms to improve ecological protection efficiency.

Key words: ecological land; Guangdong-Hong Kong-Macao Greater Bay Area; spatial-temporal evolution; anthropogenic-natural factors; interaction effect; geographical detector

1 Introduction

An urban agglomeration can be defined as a spatially compact and economically highly integrated cluster of cities (Fang and Yu, 2017). Mega-urban agglomeration (or urban megaregion) physically cover not only the spatially proximal urban areas with different scales but also the intervening suburban and exurban regions, which are linked by social processes, including population migration, policy initiatives and lifestyle changes (Seto et al., 2012). Ecological land is an important requirement for the sustainable development of urban agglomerations (Meyfroidt et al., 2018; Peng et al., 2017) through maintaining ecological security, beautifying the environment and contributing to society's physical and mental health (Markevych et al., 2017). However, the problem of ecological land destruction is increasingly prominent in response to the amplified effects of environmental change and anthropogenic disturbance (Deng et al., 2015). Over the past forty-odd years, mega-urban agglomeration in China has exhibited extensive urban population growth and urban sprawl, which brought significant negative impacts on ecosystem services (Costanza

et al., 2014; Qiu et al., 2019). As one of the most open and economically vibrant mega-urban agglomerations in China and even the world, the Guangdong-Hong Kong-Macao Greater Bay Area (GBA) is playing an increasingly important role in economic globalization and national development (Hui et al., 2018). However, the sprawl of urbanisation in the GBA has led to problems such as vegetation degradation, landscape pattern fragmentation, ecological function decline, which aggravate the conflict between human and environment (Yang et al., 2019), and may have a profound impact on the future development of GBA. Thus, there is a great need to optimize the spatial allocation of ecological land in urban agglomerations (Luo et al., 2020).

Previous scholars have extensively explored ecological land, with particular emphasis on the following research areas: (1) spatial-temporal evolution and optimization of ecological land spatial patterns and (2) analysis of ecological land influencing factors and mechanisms based on land use/cover. In the first case, some researchers have used ecological network theory (Zhang et al., 2020), landscape connectivity (Guo et al., 2020) and landscape indices (Li et al., 2020; Qiu et al., 2019) to evaluate ecological spatial patterns. For example, Serret et al. (2014) explored the distribution of Green Spaces at Business Sites (GSBS) in Paris and evaluated its contribution to the regional ecological network. Results showed that the entire Green Space network connectivity increased because 23% of the GSBS patches acted as stepping stones for mobile species. Soltanifard and Jafari (2019) assessed the ecological quality of Mashhad, Iran, and found that ecological patches that did not

possess adequate extent and continuity do not effectively support some of the key ecosystem services. Other studies pointed to ecological land fragmentation (Atasoy, 2018; Peng et al., 2017) as a factor that facilitates a reduction in the value of ecosystem services (Chen et al., 2020; Long et al., 2014), which subsequently triggers the urban heat island effect (Scolozzi and Geneletti, 2012) and other ecological safety hazards.

With respect to the second research focus, ecological land is collectively affected by natural and anthropogenic factors (Xie et al., 2017). Elevation and slope are considered to be the general limiting natural factors for ecological lands, with flatter, lower elevation ecological areas being more susceptible to development as agricultural and urban land (López-Barrera et al., 2014; Peng et al., 2017). Climatic and hydrological conditions (Smith et al., 2019), as well as soil organic matter content (Xie et al., 2017), are also associated with changes in ecological land. Anthropogenic factors have contrasting impacts on ecological land. Specifically, urban expansion (Peng et al., 2017), population growth, economic development (Li et al., 2020), and agricultural production (Tilman et al., 2002) have negative effects on ecological land, such as encroaching out ecological space and destroying ecosystem diversity (Deng et al., 2015). Additionally, as the standard of living improves, managers and citizens are increasingly concerned about the recreational benefits of green space and are demanding more ecological land in the city (Xie et al., 2014; Yang et al., 2020). Methodologically, previous studies used graph theory model (Serret et al., 2014), regression analyses (López-Barrera et al., 2014; Peng et al., 2017; Xie et al., 2014)

and spatial econometrics models (Xie et al., 2017; Yang et al., 2020) to analyze the linear relationship of driving factors on ecological land, and explored the mechanism in combination with the research area. The geographical detector has been proposed by Wang et al. (2010) to quantify the contribution of factors to dependent variables based on spatial stratified heterogeneity. This method has shown good performance and is widely used to quantify the influence of the factors that determine the spatial patterns of ecological land (Chen et al., 2020; Hu et al., 2020).

While certainly insightful, existing studies have failed to address three primary issues. First, current research on ecological land focus on the urban scale, while the regional integration analysis of the ecological land's spatial-temporal changes in urban agglomeration is still lacking. Second, there are significant spatial-temporal heterogeneous in the effect of driving factors on ecological land (Zhang et al., 2018), but few studies have explored the variation and mechanisms of driving factors' impact over time. Further, most of the research usually focuses on the unilateral role of driving factors, and rarely explores the interaction effects between factors. Third, many land cover datasets are publicly available with spatial resolution ranging from 30 m to 1 km, but the production of these datasets is still relying on manual intervention, making it difficult to update land use/cover database over long time series (Hu and Hu, 2019; Midekisa et al., 2017). The way of processing long-term land use/cover remote sensing data needs to be improved by using some effective methods (Zhang et al., 2017).

To solve the issues mentioned above, here we investigated the spatial-temporal

patterns of ecological land in the GBA, as well as the effect of driving factors combining natural and anthropogenic data based on 30m land use/cover data from 1990-2019. Specifically, this paper focused on three issues: (1) What are the changing characteristics and trends of ecological land distribution in the GBA over the past 30 years? (2) What are the natural and anthropogenic forces that affect ecological land, and how do their interactive effects and influence mechanisms behave? (3) What are the characteristics of the temporal changes of these driving factors' effect?

2 Material and methods

2.1 Study area

According to the *Outline Development Plan for the Guangdong-Hong Kong-Macao Greater Bay Area* published by the Chinese government in 2019, the GBA should not only become a world-class mega-urban agglomeration but also create a good-quality region suitable for working, living and traveling (Wang et al., 2020). The GBA consists of the Hong Kong Special Administrative Region (HK), the Macao Special Administrative Region (MC) as well as 9 prefecture-level cities, namely Guangzhou (GZ), Shenzhen (SZ), Zhuhai (ZH), Foshan (FS), Huizhou (HZ), Dongguan (DG), Zhongshan (ZS), Jiangmen (JM) and Zhaoqing (ZQ) in the Pearl River Delta (PRD), with a total area of 56,904 km^2 (Fig. 1). There are different levels of economic and social development and political systems within the GBA. In 2019, the total GBA resident population was 72.7 million, the urbanization rate was 86.1%, the GDP was $11,591 billion, and the tertiary industry accounted for 66.4% of the

GDP. The GBA is an urbanized area with a high level of integration. Rapid urbanization and high intensity land development in the GBA generated considerable pressure on regional ecological land protection (Zhou and Mu, 2019), making ecological conservation a policy concern (Table A1). Thus, identifying and understanding the evolution and formation mechanism of the GBA's spatial pattern of ecological land has become a valuable fundamental research work for regional ecosystem governance.

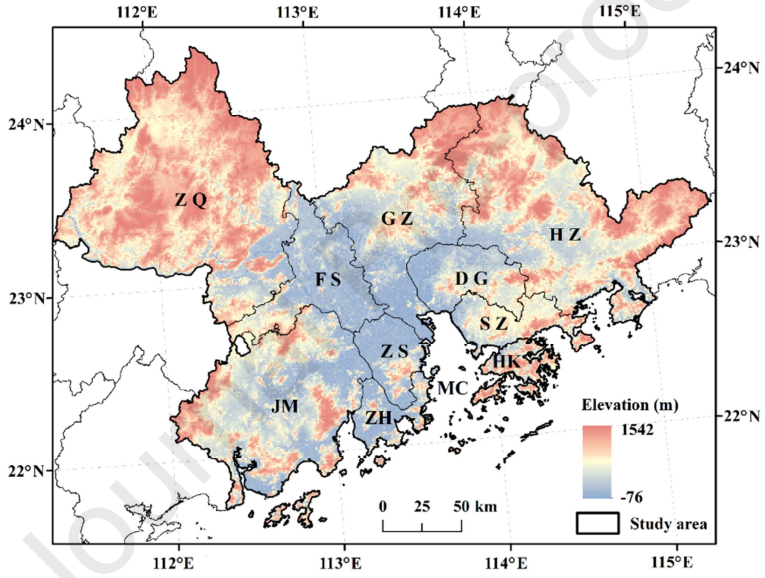

Fig. 1 Topography map of the Guangdong-Hong Kong-Macao Greater Bay Area (GBA). The GBA includes 11 cities: Guangzhou (GZ), Zhaoqing (ZQ), Foshan (FS), Dongguan (DG), Huizhou (HZ), Jiangmen (JM), Zhongshan (ZS), Shenzhen (SZ), Zhuhai (ZH), Hong Kong (HK), and Macao (MC).

2.2 Data sources

According to the definition of ecological land in the *Opinions on the Delineation and Strict Observance of the Red Line of Ecological Protection* (Hu et al., 2020), land use types in the study area were classified as either ecological (forest, grassland, and water) or non-ecological (construction and other land), agricultural land is excluded

from the ecological land. The Google Earth Engine (GEE) has supplied a platform that provides basic calculation functions for raster and vector data and can be used by developers (Gorelick et al., 2017; Hu and Hu, 2019). Therefore, the data used included available standard Level 1 Terrain-corrected (L1T) orthorectified surface reflectance images of the 1990-2019 plant growing seasons from Landsat TM/ETM+/OLI archived in the GEE. We also use the land-use dataset interpreted by Resource and Environment Data Cloud Platform (RESDC) (http://www.resdc.cn), which is characterized as highly accurate by field survey and random sampling check which were conducted by Chinese Academy of Sciences (Chen et al., 2020). In addition, based on a literature review in section 1 and data accessibility, elevation (DEM), slope (Sp), average annual precipitation (Tem), average annual temperature (Pre), population density (POP), GDP per capita (GDPPC) and land urbanization rate (LUB) were selected as driving factors (Table A2).

2.3 Research procedure

The research framework was divided into six steps (Fig. 2):

(1) With the support of the GEE, the multiyear image synthesis and cloud mask methods (Zhu et al., 2015) were applied to obtain the TOA composite data without cloud or shadow coverage, for each year from 1990-2019. These images were subsequently cropped according to the study area boundary;

(2) Using the Land cover dataset, training and verification samples were carefully deployed according to the “complete consistency” and “temporal stability” principles. Then, the land cover dataset was reclassified into the same land types.

Pixels with completely consistent, unchanged land cover types were selected, while 3206 training pixels and 1,202 validation pixels, were randomly selected to ensure a minimum of 200 validation pixels per land use type;

(3) There are many automatic land classification algorithms, such as minimum distance classification (MDC), random forest (RF), maximum likelihood classification (MLC), classification and regression trees (CART), support vector machine (SVM), and object-oriented classification methods (Gómez et al., 2016). Among these algorithms, the RF method, formed by a combination of many decision tree models, is widely used (Breiman, 2001; Hu and Hu, 2019). In addition, compared with traditional land classification algorithms, the RF method has obvious advantages in multidimensional feature data processing. Previous studies also have verified that RF model training is an effective classification method (Ou et al., 2019). Therefore, we chose the RF as a classifier with ensembles of 500 trees to obtain the land cover classification maps for each chosen year based on Landsat satellite images and auxiliary data. For more details about the auxiliary data processing, see Appendix A;

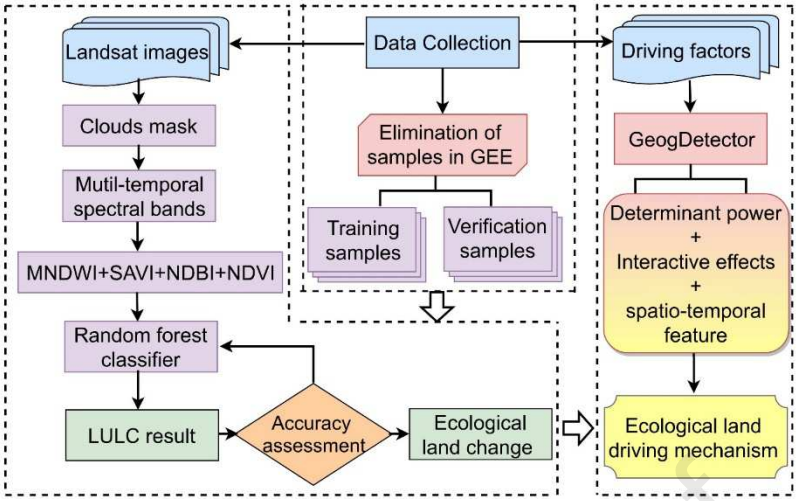

Fig. 2 Flowchart of land cover mapping and mechanism analysis. Note that MNDWI, SAVI, NDBI and LULC represent Modified Normalized Difference Water Index (MNDWI), Soil Adjusted Vegetation Index (SAVI), Normalized Difference Built-Up Index (NDBI) and land use/cover.

(4) The overall accuracy and kappa coefficient were calculated from the error matrix (Hu and Hu, 2019; Sun et al., 2018) to evaluate the classification results accuracy by using the RESDC land cover dataset as the standard. The overall accuracy and the Kappa coefficient of the study area's land cover classification (Fig. 3) from 1990-2019 was 0.93±0.05 and 0.89±0.04 (Table 1), respectively, which met the research requirements. The output images were further converted into ecological land and non-ecological land;

(5) Land use change matrix and four indicators were selected to analyze changes in the GBA's landscape pattern of ecological land (Table A3). The indicators include Edge Density (ED), Patch Density (PD), Contagion Index (CONTAG), and Shannon's Diversity Index (SHDI), all of which were calculated by Fragstats 4.1 (Thapa and Murayama, 2009). ED indicates the smoothness of patch edges and PD reflects the fragmentation and anthropogenic disturbances on the landscape. CONTAG refers to

the agglomeration of different patch types, which is an index used to describe the spatial information of a certain landscape pattern. The SHDI reflects the landscape heterogeneity, where higher values correspond to more patch types;

(6) Elevation and construction land data were used to calculate slope and land urbanization rates, respectively. A geographic detector was used to investigate the forces, interactions, spatial-temporal characteristics, and influence mechanism of natural and anthropogenic factors on the evolution of ecological land.

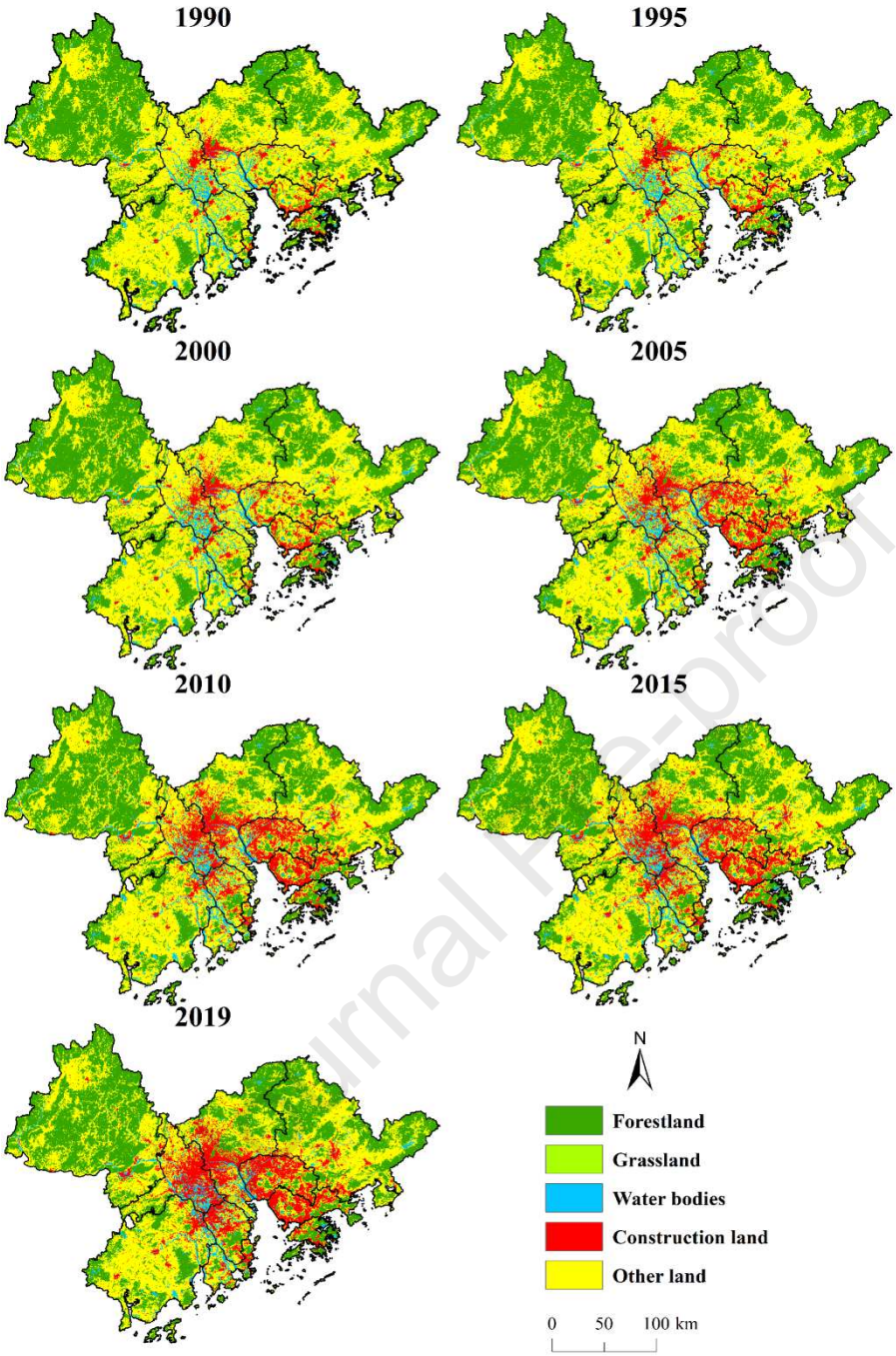

Fig. 3 Land cover maps in the Guangdong-Hong Kong-Macao Greater Bay Area during 1990-2019

Tab. 1 Overall accuracy assessment of land use classification from 1990-2019

	Forestland	Grassland	Water bodies	Construction land	Other land	Overall
Kappa coefficient	0.87±0.03	0.86±0.02	0.92±0.03	0.90±0.05	0.88±0.09	0.89±0.04
Accuracy	0.90±0.03	0.91±0.02	0.96±0.02	0.94±0.06	0.90±0.08	0.93±0.05

2.4 Geographical detector

The geographical detector can capture the spatial relationship between the driving factors and the distribution of ecological land, as well as the interactions between the driving factors. When there is a nonlinear relationship between an explained variable and explanatory variables, this method is more applicable than a linear model (Wang et al. 2016). We assumed that the ecological land has a spatial distribution similar to that of a driving factor if the impact factor leads to the observed distribution of ecological land (Wang et al., 2010; Wang et al., 2016). The geographical detector comprises four modules: factor, interaction, risk, and ecological detectors. Factor detector, interaction detector and risk detector are mainly used in the current study. The factor detector uses a q value to quantify the influences of variable X on Y; q is determined by the following formula:

$$q = 1 - \frac{\sum_{h=1}^{L} N_h \sigma_h^2}{N\sigma^2} = 1 - \frac{SSW}{SST},\ SSW = \sum_{h=1}^{L} N_h \sigma_h^2,\ SST = N\sigma^2 \quad (1)$$

where q is the power of the determinant; N and N_h are the number of sample units in the entire region and sub-region; h=1,2…, L is the number of secondary regions; σ_h and σ^2 are the variance of the samples in subregion h and the global variance of Y over the entire study region. SSW and SST are the within sum of squares and the total sum of squares, respectively. The value range of q is [0,1], this means the selected driving factor explains $q \times 100\%$ of the explained variable. The larger the q value, the stronger the influence of variable X on Y.

The ecological detector is used to compare whether $X1$ has a significantly greater

influence or contribution than *X2*. It is measured using the statistics *F*:

$$F = \frac{N_{X1}(N_{X2}-1)SSW_{X1}}{N_{X2}(N_{X1}-1)SSW_{X2}},\ SSW_{X1} = \sum_{h=1}^{L1} N_h \sigma_h^2,\ SSW_{X2} = \sum_{h=1}^{L2} N_h \sigma_h^2 \quad (2)$$

where $N_{X1}$and N_{X2} represent the number of factors *X1* and *X2* samples; $SSW_{X1}$and SSW_{X2} are the within sum of squares in the subregion generated by factor layers *X1* and *X2*. *L1* and *L2* represent the number of *X1* and *X2* subregions. The null hypothesis is defined as H_0: $SSW_{X1} = SSW_{X2}$. The rejected H_0 at the significance level indicates that it is statistically significant.

The interaction detector examines the interaction of different factors and reveals whether the interaction of factors *X1* and *X2* weaken, enhance, or are independent of influencing *Y*. The interactive relationship can be divided into five categories by comparing the interactive *q* value of the two factors and the *q* value of each of the two factors (Table 2).

Tab. 2 The interactive categories of two factors and the interactive relationship

Description	Interaction
$q(X1 \cap X2) < Min(q(X1), q(X2))$	Weaken; univariate
$Min(q(X1), q(X2)) < q(X1 \cap X2) < Max(q(X1), q(X2))$	Weaken; univariate
$q(X1 \cap X2) > Max(q(X1), q(X2))$	Enhanced, bivariate
$q(X1 \cap X2) = q(X1) + q(X2)$	Independent
$q(X1 \cap X2) > q(X1) + q(X2)$	Nonlinearly enhance

3 Results and discussions

3.1 Temporal evolution characteristics of ecological land in the GBA

In 1990, ecological land in the GBA accounted for 26,716.14 km^2, 47.19% of the total area. Forestland, water body and grassland comprised 22208.58 km^2, 3,094.11

239 km^2, and 1,413.45 km^2 respectively. From 1990-2000, the total ecological land area
240 decreased by 485.1 km^2, and grassland decreased by 397.35 km^2, accounting for
241 81.91% of the total reduction (Fig. 4a). From 2000-2010, ecological land area rapidly
242 diminished by 899.46 km^2, mainly in grassland (543.6 km^2) and water bodies (156.33
243 km^2). The period of 2010-2019 demonstrated slow growth in the ecological land area
244 with an increase of 15.21 km^2, of which forest land increased the most (223.74 km^2),
245 while water body and grassland decreased by 21.69 $km^2$and 186.84 km^2, respectively.
246 In summary, from 1990-2019, the ecological land in the GBA decreased from 47.19%
247 to 44.77% (1,369.35 km^2). Specifically, the forestland area increased by 5.85 km^2
248 (0.03%); while grassland and water bodies decreased by 1127.79 km^2 (79.79%) and
249 247.41 km^2 (8%), respectively. The GBA exhibits the typical conflict between urban
250 sprawl and ecological land conservation (Wang et al., ,2020).

251 From 1990-2019, the ecological land in the GBA underwent severe destruction
252 and gradual recovery, with a landscape pattern characterized by fragmentation
253 followed by integration (Fig. 4b). Specifically, from 1990-2010, ED and PD increased
254 by 9.72% and 12.02%, respectively, indicating more irregular ecological land patch
255 edges and more intense landscape fragmentation; CONTAG and SHDI decreased by
256 16.04% and 17.06%, respectively, demonstrating that the fragmentation of ecological
257 land has caused a rapid decline in landscape diversity. However, from 2010-2019, ED
258 and PD decreased by 2.21% and 1.27%, signifying that the ecological land patch
259 edges had become regular and continuous; CONTAG and SHDI increased by 2.61%
260 and 0.63%, suggesting that there was a tendency of spatial agglomeration with respect

261 to ecological land distribution that improved landscape diversity.

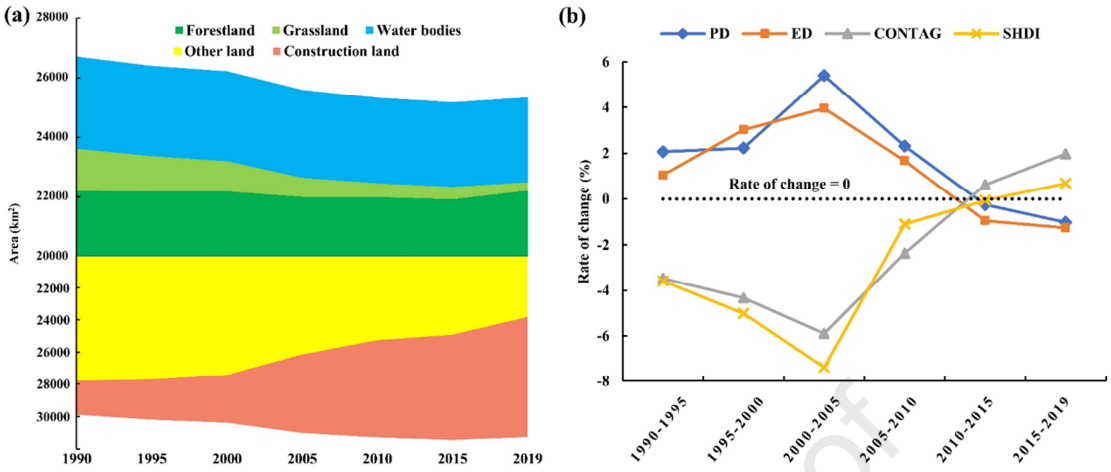

Fig. 4 Land cover area change(a) and ecological land landscape metrics change (b): Patch Density (PD), Edge Density (ED), Contagion Index (CONTAG), and Shannon's Diversity Index (SHDI)

262 3.2 Spatial evolution characteristics of ecological land in the GBA

263 The evolution of ecological land distribution in the GBA generally shows a
264 process of decreasing in the central area (Fig. 3). Ecological land was concentrated on
265 the periphery of GBA, with forestland and grassland mainly distributed in
266 northeastern GZ, northwestern ZQ, and eastern and northern HZ. Water bodies were
267 scattered in FS, ZH and DG. In addition, the average proportion of MC's ecological
268 land was only 29.17% and the proportion of ecological land in HK (57.47%) and ZQ
269 (62.95%) is much higher than the regional average (45.76%) (Table A4), which is
270 closely related to location, urbanization development stage, and local policies. For
271 example, as a Special Administrative Region, HK is highly urbanized but with a land
272 policy that strictly protects ecological land (Hasan et al., 2019; Wong et al., 2017).
273 The urbanization rate of ZQ is only 48.63%, while the forest coverage rate is over
274 70%, making it the main forest area in GBA.

From 1990-2000, 306.54 km^2 of ecological land, which was primarily concentrated on the periphery of urban built-up areas, was converted to construction land (Fig. 5 and Table A5). This was mainly due to the demand for urban construction, and resulted in partial occupation of the forestland and grassland. In addition, 492.29 km^2 of other land was converted to ecological land, mostly sporadically in ZQ and HZ, likely in response to the "returning slope farmland to forest, grass and water" policy enacted in 1998 (Long et al., 2012). From 2000-2010, due to rapid urbanization and industrialization, 1,476.1 km^2 of ecological land in industrialized cities, such as SZ, FS and DG, was converted for construction and other land use purposes (Table A5). From 2010-2019, ecological land area in the GBA experienced numerous fluctuations, but overall showed an increasing trend. 659.26 km^2 of non-ecological land, mainly distributed in GZ and HZ, was converted to ecological land (Table A5), which was likely in response to Guangdong's urban greening initiative (The People's Government of Guangdong Provence, 2013), the implementation of "ecological red line (an important tool for ensuring development of environmentally sustainable communities)" (Hu et al., 2020), as well as major natural ecosystem protection and comprehensive land improvements projects (Long et al., 2014). These efforts collectively and effectively decelerated the decrease of ecological land space. However, 404.94 km^2 of ecological land was still converted to non-ecological land which is mainly composed of cash crops planting areas and urban construction land. Thus, ecological land still requires significant additional protective measures.

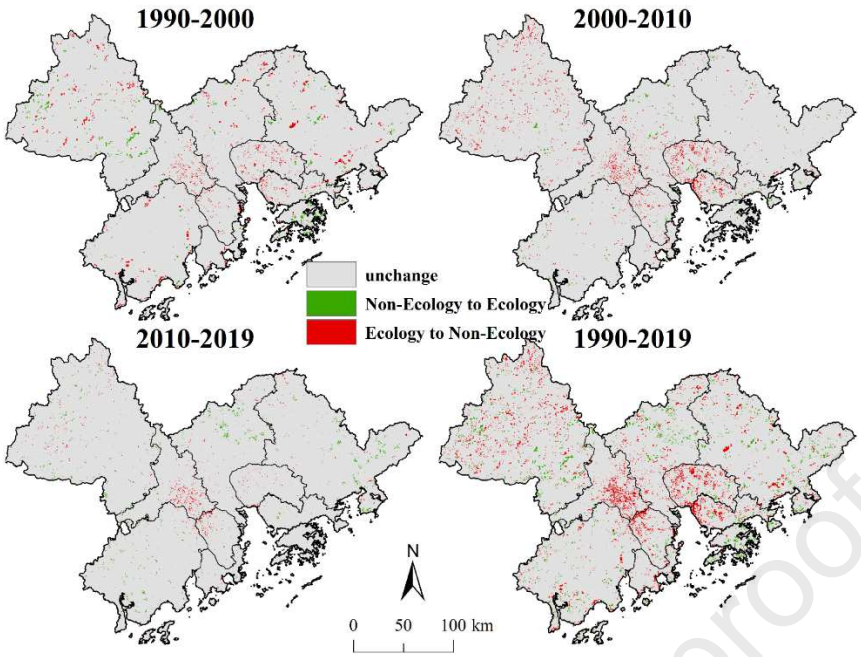

Fig. 5 Spatial transition pattern of ecological land in the Guangdong-Hong Kong-Macao Greater Bay Area

296 3.3 Driving factors' effect on the spatiotemporal evolution of ecological land

297 The geographical detector was used to calculate each factor's force on ecological
298 land evolution form 1990-2019. Based on the power of determinant on spatial
299 heterogeneity, the driving factors can be ranked as follows: POP > LUB > GDPPC >
300 DEM > Sp > Tem > Pre (Fig. 6). Except for Pre and Tem, the other driving factors
301 were statistically significant at the 1% level. Moreover, anthropogenic factors had a
302 generally greater influence on ecological land than natural factors, which is consistent
303 with several published studies (Peng et al., 2017; Wang et al., 2018; Xie et al., 2017).
304 In addition, there are statistically significant impact differences between 47.6% of the
305 driving factors' interaction (Fig. 6).

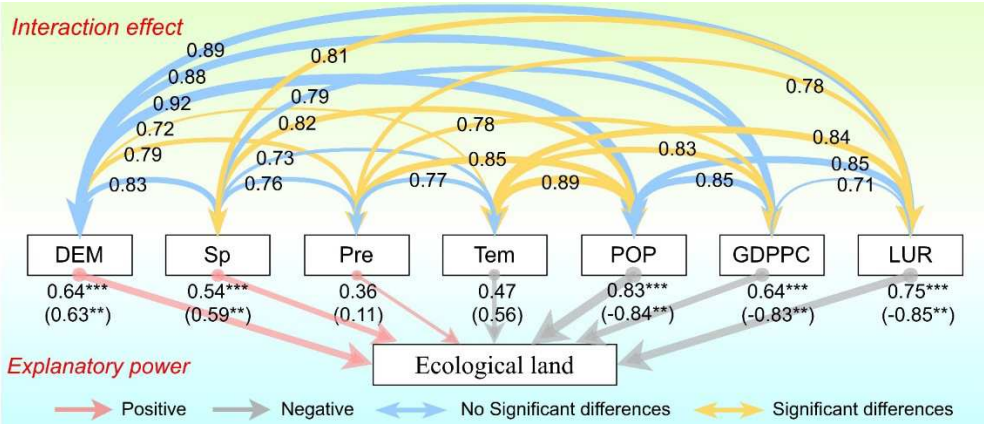

Fig. 6 The determinant and interaction power of driving factors on ecological land. *** and * * indicate significance at the 1%, 5% levels, respectively; the thickness of the line represents the strength of the influence or interaction; the abbreviations of factors are listed in Section 2.2

306 For the anthropogenic factors, POP and LUR had a significant negative effect on
307 ecological land in the GBA, with *q* values of 0.83 and 0.75, respectively. It is similar
308 to the finding in previous studies which also demonstrated that population increase
309 was the key factor facilitating significant decline of ecological land (Xie et al., 2017).
310 The GBA resident population reached 72.7 million in 2019, which was 2.46 times that
311 in 1990. The massive population density in the cities led to an increasing demand for
312 construction land (e.g., housing, transport, industry), and resulted in a large amount of
313 ecological land being converted and occupied; thus, exacerbating the conflict between
314 social development and ecological protection (Long et al., 2014). Meanwhile, the
315 GDPPC determines 64% of the ecological land distribution, and has a significant
316 negative effect, indicating that high economic density areas are mostly urban cores,
317 and their proportion of ecological land is also generally low (Peng et al., 2017; Wang
318 et al., 2018). For natural factors, DEM and Sp were positively correlated with
319 ecological land, with *q* values of 0.64 and 0.54, respectively. Consistent the findings

in previous studies, topography play an important role in ecological land (Smith et al., 2019; Xu et al., 2019). Ecological land with flat slopes and lower elevation are more likely to be exploited for agriculture and urban land (López-Barrera et al., 2014; Newman et al., 2014; Xie et al., 2017), as higher altitudes correspond with higher development cost. However, cities in GBA are influenced by the typical East Asian Monsoon (EAM), with irregular fluctuations in annual precipitation and temperature (Hallegatte et al., 2013; Luo et al., 2019; Piao et al., 2003). It is observed that the causal relationship between the change trend of temperature, rainfall and ecological land is not obvious, which weakens the explanatory power of Pre (0.36) and Tem (0.47) on ecological land evolution.

The interactive relationship between each pair of factors was bivariate, and thus enhanced each other in influencing ecological land (Fig. 6). Among the interactions between anthropogenic and natural factors, q(POP∩DEM) was the maximum (0.92), indicating that the coupling between POP and DEM is the key to influencing ecological land evolution. As the POP and DEM have great effects on the distribution of ecological land, their interactive effect is also very prominent.With respect to interactions among anthropogenic factors, q(POP∩LUR) and q(POP∩GDPPC) were the strongest (0.85). In regions with high populations and economic development, ecological land is more easily converted into construction land (e.g., residential buildings and commercial industry), which can generate greater profits and better stimulate the local economy. Among the natural factor interactions, q(DEM∩Sp) exhibited the maximum value (0.85). Low, flat areas make it easier to convert

342 ecological land into construction land. Mountainous areas, with their high elevation
343 and undulating terrain, have hydrothermal and other conditions that make them
344 unsuitable for most anthropogenic activities, but conducive to vegetation growth and
345 ecological land protection.

346 Figure 7(a) shows the distribution of the driving factors on the ecological land
347 evolution during 1990-2019. Apparently, the spatial distribution of dominant factors
348 was heterogeneous in the GBA, presenting a pattern dominated by anthropogenic
349 factors in the central part (e.g., ZS, FS, ZH, SZ and DG) and transitioning to a pattern
350 dominated by intersection of anthropogenic-natural factors in the periphery (e.g., GZ,
351 ZQ, JM, and HZ). In addition, the regions of Pre and Tem determinant were relatively
352 small, scattered in northern GZ, eastern HZ and western JM. After sequencing the
353 cities according to population density from high to low (Fig. 7b), it can be seen that
354 the higher population density of a city, the more sensitive the ecological land
355 evolution is to anthropogenic factors. POP and LUR determined 28.6% and 26.5% of
356 the ecological land evolution, respectively, while GDP and DEM accounted for 16.3%
357 and 10.2%, respectively, much more than Sp (8.2%), Tem (6.1%) and Pre (4.1%) (Fig.
358 7c). Therefore, anthropogenic activities dominate the evolution of ecological land in
359 the GBA, which is consistent with previous study (Yang et al., 2019).

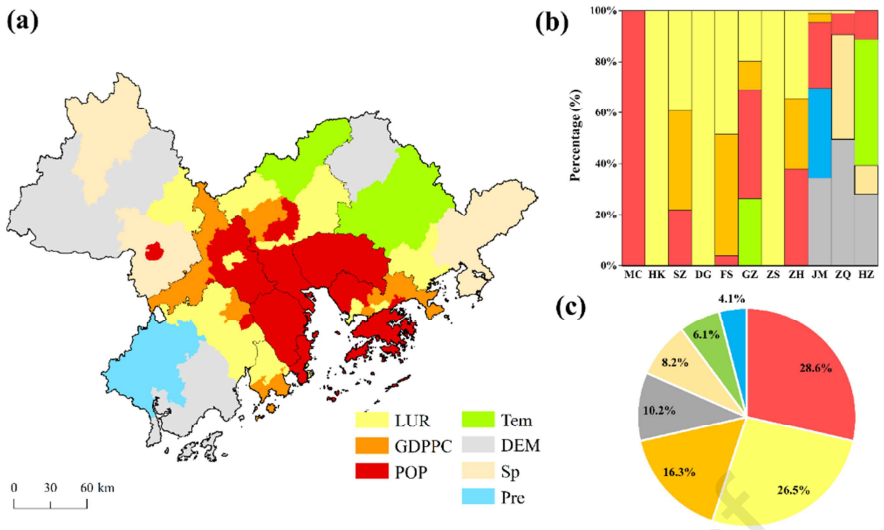

Fig. 7 (a) Spatial pattern of determinant driving factors on the ecological land evolution, (b) Area percentage of determinant driving factor of all cities, and (c) the number proportion of driving factors on the whole study region. Abbreviations are defined in Fig. 1 and Section 2.2

3.4 Dynamic changes of driving factors' effect on ecological land

The driving factors' influence (*q* values) on ecological land evolution from 1990-2019 were calculated using the factor detector and are presented in Table 3. For anthropogenic factors, GDPPC and PD were more stable than LUR (Fig. 7a). The *q* values of POP and GDPPC increased by 36.8% and 23.4%, respectively, indicating that the two factors had an increasing marginal effect on the ecological land. The correlation between GDPPC and ecological land decreased from -0.88 to -0.78, demonstrating that the negative effect between economic development and ecological land gradually weakened. Essentially, with the urban landscape planning optimization, regions with a high GDPPC and urbanization rate are more likely to pursue a higher quality living environment; thus, green space coverage is relatively high. For example, HK effectively protected ecological land and the value of ecological services through policies such as the *Town Planning Ordinance*, which was designed to promote

conservation and protection of country parks, coastal protection areas, and green belts (Wong et al., 2017). SZ and GZ also used green space landscape planning (e.g., green space connectivity design) to achieve the growth of ecological land within the built-up areas (Peng et al., 2017). However, the effect of LUR on ecological land is characterized by a gentle decrease followed by an increase, possibly due to the fact that the GBA's industrial structure shifted from a secondary industry to a tertiary industry from 1990-2005. The tertiary industry increased from 41.6% to 56.6% (Fig. 7b), which reduced the destruction of ecological land by industrialization-led urban sprawl. In contrast, from 2005-2019, the large migrant influx in the GBA (the resident population grew by 1996.64 million) led to a sharp increase in demand for housing, education, medical services, and other facilities (Wang et al., 2020), which directly promoted urban sprawl and the occupation of surrounding ecological land (Fig. 4). LUR gradually became the main driving factor on ecological land evolution.

Tab. 3 Determinant Power (*q* value) of driving factor on ecological land from 1990-2019

Year	DEM		Sp		Pre		Tem		POP		GDPPC		LUR	
	q	*ρ*	*q*	*ρ*	*q*	*ρ*	*q*	*ρ*	*q*	*ρ*	*q*	*ρ*	*q*	*ρ*
1990	0.63***	0.64**	0.52***	0.56**	0.57***	0.11	0.59***	-0.47**	0.57***	-0.78**	0.64***	-0.88**	0.84***	-0.85**
1995	0.63***	0.64**	0.53***	0.56**	0.67**	-0.33**	0.59***	-0.52**	0.72***	-0.77**	0.61***	-0.87**	0.60***	-0.85**
2000	0.63***	0.65**	0.54***	0.58**	0.37***	-0.24	0.67***	-0.62**	0.62***	-0.79**	0.67***	-0.87**	0.51***	-0.84**
2005	0.64***	0.66**	0.55***	0.59**	0.19**	0.07	0.73***	-0.63**	0.61***	-0.80**	0.71***	-0.87**	0.65***	-0.85**
2010	0.64***	0.68**	0.55***	0.61**	0.18	0.01	0.58***	-0.62**	0.74***	-0.87**	0.76***	-0.73**	0.76***	-0.87**
2015	0.64***	0.69**	0.54***	0.62**	0.20	0.23	0.19	-0.16	0.71***	-0.84**	0.73***	-0.75**	0.76***	-0.87**
2019	0.65***	0.70**	0.56***	0.63**	0.13	0.17	0.18	-0.15	0.72***	-0.80**	0.79***	-0.78**	0.77***	-0.87**

*** and * * indicate significance at the 1%, 5% levels.

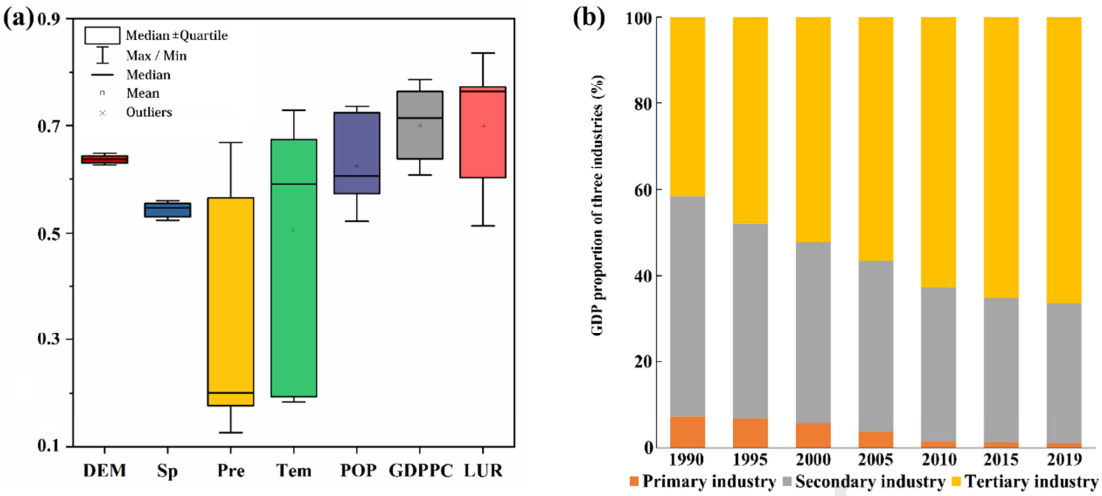

Fig. 8 (a) The box-whisker plot of *q* values for driving factors and (b) the changes of industrial structure over 1990 to 2019

For natural factors, the *q* values of Tem and Pre were relatively high at the very beginning, then decreased from 0.59 to 0.18 and 0.57 to 0.13, respectively, implying a gradual weakening of the impact these two factors exert on ecological land. It may because the disturbance of anthropogenic activities, especially the regional planning and policies, on the distribution of ecological land is gradually increasing (Xie et al., 2017). For example, from 2010-2019, the GBA issued five ecological conservation policies (Table A1), leading to the construction of arge areas of green space. Park green space with a 500 m radius covered every corner of the city. At the same time, this stage is still a period of rapid urban expansion (Fig. 4), made LUR's impact on ecological land continuously increase (Yang et al., 2019). Based on the above, it can be observed that the effects of these human factors have been increasing, while the influence of Tem and Pre on the ecological land evolution has been weakening. However, from the scale of the entire urban agglomeration, the macro pattern of DEM and Sp has a fundamental role in the formation of the ecological landscape pattern in

GBA, and their effects on ecological land were essentially stable over time (Fig. 7a).

4 Conclusions and implications

4.1 Conclusions

(1) Ecological land evolution in the GBA exhibited prominent spatial-temporal heterogeneity, and its distribution experienced a shift from decline and fragmentation (1990-2010) to growth and integration (2010-2019). From 1990-2010, the proportion of ecological land in the whole region decreased from 47.19% to 44.75%, a decrease in area equivalent to 1384.56 km^2 and the landscape of ecological land was more fragmented and irregular. From 2010-2019, the ecological land area with an increase of 15.21 km^2, and there was a tendency of spatial agglomeration with respect to ecological land distribution. Moreover, ecological evolution pattern of the GBA underwent a process of decreasing in the central area, with 82.4% of the ecological land converted to construction land during the study period, which was mainly distributed in and around the built-up areas of FS and ZQ.

(2) Anthropogenic-natural factors and their interactions had significant influence on the ecological land. From a long-term perspective, the impact of anthropogenic factors (with POP being the major factor; q=0.75) on ecological land was generally greater than that of natural factors. Moreover, the interaction effects among the factors were bivariate, and the interaction between elevation and population density was the largest (q =0.92). Importantly, the spatial distribution of dominant factors was heterogeneous, presenting a pattern dominated by anthropogenic factors in the central

part and transitioning to a pattern dominated by intersection of anthropogenic-natural factors in the periphery.

(3) The effect of anthropogenic-natural factors on ecological land evolution is dynamically changing. The impact of POP and GDPPC showed a significant upward trend during the study period (the *q* values increased by 36.8% and 23.4%, respectively). However, the impact of LUR was characterized by gradual decrease and then increase, which paralleled industrial restructuring and accelerated urbanization. It is noteworthy that under the combined influence of anthropogenic activities (e.g., policy planning, urban expansion, and public concern), the influence of natural factors on ecological land gradually weakened (the *q* values of Tem and Pre declined by 69% and 77%, respectively).

4.2 Policy implications

(1) In the GBA, where the impact of anthropogenic activities on the surface environment is more intense, the ecological land driving force is more complex. The coupling relationship between anthropogenic and natural factors requires special consideration when addressing ecological land protection; and slow but steady change for ecological land's spatial pattern should be promoted through adjustment of these combined of factors. Our findings indicated that population migration in high-altitude areas and rational population distribution and afforestation in low-altitude areas are important initiatives for ecological land protection. The development and implementation of ecological land policies (Table 1) in some cities in the GBA accelerated urban greening, major natural ecosystem protection and comprehensive

444 land improvements projects.

445 (2) The impact of driving factors on ecological land evolution in the GBA have
446 significant differences over time. Therefore, policymakers need to formulate diverse
447 policies at different periods and in various cities. For example, population growth and
448 economic development have gradually increased the impact of ecological land, so
449 special attention should be paid to population evacuation and rational industrial layout
450 of core cities (e.g. SZ, HZ and ZS). In addition, for cities adjacent to the GBA core
451 area (e.g. ZH), we should also be alert to the volatile impact of urbanization on the
452 ecological land degradation and landscape fragmentation, and restrict the disorderly
453 expansion of construction land. Furthermore, due to the stability of the topography's
454 impact, elevation and slope also should be considered when designing ecological
455 conservation and planning. Of course, climate conditions were also the main factors
456 affecting ecological land in GBA's peripheral cities (e.g., HZ and JM), but the forces
457 were constantly decreasing. Therefore, for these cities, it is necessary to minimize the
458 intervention of human activities and explore the driving mechanism of climate change
459 on ecological land.

460 (3) The spatial distribution of dominant driving factors of the ecological land
461 evolution in the GBA presents obvious regional and intercity relevance. With the
462 growing close spatial connection within the GBA, the joint governance of ecological
463 spaces across cities should been greatly enhanced, ultimately realized regional-scale
464 ecological land restoration. In addition, the GBA should establish a new mechanism
465 for more effective regional ecological land protection and coordinated development,

implement multi-city planning integration to reduce the fragmentation and degradation of ecological land. Moreover, the focus of land policy formulation should be shifted from simply improving the land's productive function and economic value to improving its ecological function.

4.3 Innovations and limitations

This work takes the lead in examining the evolutionary characteristics of long-term ecological land series in the GBA, and considers the interaction and dynamic change of driving factors' effect on ecological land evolution. The data derived from this investigation are valuable reference for enriching the existing analytical framework and establishing ecological protection policy. In addition, with respect to methodology, this study used a geographical detector to eliminate the problem of multicollinearity among drivers, and quantify the forces of ecological land evolution. Furthermore, the nominal overall accuracy of publicly available land use/cover products ranges from 60–80%, which cannot meet the needs of environmental monitoring and ecological governance and reduces the accuracy and credibility of small and medium-scale studies (Zhao et al., 2014). The remote sensing processing method based on long-term Landsat satellite imagery and other auxiliary data supported by the GEE platform is used for efficient and accurate mapping of land use/cover, which provides an effective alternative for land mapping.

This study also has some limitations. First, ecological land is influenced by a variety of factors, and more driving factors should be selected to explore the mechanisms of ecological land evolution further and more thoroughly. Secondly, there

488 are differences in the driving factors and influence mechanisms on ecological land
489 evolution in various cities within the GBA. Although they have been mentioned in the
490 current study, there is a lack of systematic and in-depth analysis. Future research
491 should focus on conducting a deeper, more granule comparative study of the
492 differences in the spatial-temporal patterns and drivers of ecological land evolution
493 between cities.

Acknowledgments

This study was supported by the National Natural Science Foundation of China (41901181, 41871151). We especially expressed the thanks to everyone around the world for their hard work and dedication on COVID-19. In addition, Rundong Feng wishes to thank his spiritual mentor, Kobe Bryant, whose Mamba Spirit have given his great support for the last twelve years.

References

Atasoy, M., 2018. Monitoring the urban green spaces and landscape fragmentation using remote sensing: a case study in Osmaniye, Turkey. Environ. Monit. Assess. 190, 713. https://doi.org/10.1007/s10661-018-7109-1

Breiman, L., 2001. Random Forests. Mach. Learn. 45, 5-32. https://doi.org/10.1023/A:1010933404324

Chen, T., Feng, Z., Zhao H., Wu, K., 2020. Identification of ecosystem service bundles and driving factors in Beijing and its surrounding areas. Sci. Total Environ. 711, 134687. https://doi.org/10.1016/j.scitotenv.2019.134687

Costanza, R., de Groot, R., Sutton, P., van der Ploeg, S., Anderson, S.J., Kubiszewski, I., et al., 2014. Changes in the global value of ecosystem services. Glob. Environ. Change-Human Policy Dimens. 26, 152-158. https://doi.org/10.1016/j.gloenvcha.2014.04.002

Deng, X., Yuan, Y., Wang, Z., Li, Z., 2015. Impacts of land-use change on valued ecosystem service in rapidly urbanized North China Plain. Ecol. Model. 318, 245-253. https://doi.org/10.1016/j.ecolmodel.2015.01.029

Fang, C., Yu, D., 2017. Urban agglomeration: An evolving concept of an emerging phenomenon.

Landsc. Urban Plan. 162, 126-136. https://doi.org/10.1016/j.landurbplan.2017.02.014

Gómez, C., White, J.C., Wulder, M.A., 2016. Optical remotely sensed time series data for land cover classification: A review. ISPRS-J. Photogramm. Remote Sens. 116, 55-72. https://doi.org/10.1016/j.isprsjprs.2016.03.008

Gorelick, N., Hancher, M., Dixon, M., Ilyushchenko, S., Thau, D., Moore, R., 2017. Google Earth Engine: Planetary-scale geospatial analysis for everyone. Remote Sens. Environ. 202, 18-27. https://doi.org/10.1016/j.rse.2017.06.031

Guo, X., Zhang, X., Du, S., Li, C., Siu, YL., Rong, Y., et al., 2020. The impact of onshore wind power projects on ecological corridors and landscape connectivity in Shanxi, China. J. Clean Prod. 254, 120075. https://doi.org/10.1016/j.jclepro.2020.120075

Hallegatte, S., Green, C., Nicholls, RJ., Corfee-Morlot, J., 2013. Future flood losses in major coastal cities. Nat. Clim. Chang. 3, 802-806. https://doi.org/10.1038/nclimate1979

Hasan, S., Shi, W., Zhu, X., Abbas, S., 2019. Monitoring of Land Use/Land Cover and Socioeconomic Changes in South China over the Last Three Decades Using Landsat and Nighttime Light Data. Remote Sens. 11, 1658. https://doi.org/10.3390/rs11141658

Hu, T., Peng, J., Liu, Y., Wu, J., L,i W., Zhou, B., 2020. Evidence of green space sparing to ecosystem service improvement in urban regions: A case study of China's Ecological Red Line policy. J. Clean Prod. 251, 119678. https://doi.org/10.1016/j.jclepro.2019.119678

Hu, Y., Hu, Y., 2019. Land Cover Changes and Their Driving Mechanisms in Central Asia from 2001 to 2017 Supported by Google Earth Engine. Remote Sens. 11, 554. https://doi.org/10.3390/rs11050554

Hui, ECM., Li, X., Chen, T., Lang, W., 2018. Deciphering the spatial structure of China's megacity region: A new bay area—The Guangdong-Hong Kong-Macao Greater Bay Area in the making. Cities. 105, 102168. https://doi.org/10.1016/j.cities.2018.10.011

Li, G., Jiang, C., Du, J., Jia, Y., Bai, J., 2020. Spatial differentiation characteristics of internal ecological land structure in rural settlements and its response to natural and socio-economic conditions in the Central Plains, China. Sci. Total Environ. 709, 135932. https://doi.org/10.1016/j.scitotenv.2019.135932

Long, H., Li, Y., Liu, Y., Woods, M., Zou J., 2012. Accelerated restructuring in rural China fueled by 'increasing vs. decreasing balance' land-use policy for dealing with hollowed villages. Land Use Policy. 29, 11-22. https://doi.org/10.1016/j.landusepol.2011.04.003

Long, H., Liu, Y., Hou, X., Li, T., Li, Y., 2014. Effects of land use transitions due to rapid urbanization on ecosystem services: Implications for urban planning in the new developing area of China. Habitat Int. 44, 536-544. https://doi.org/10.1016/j.habitatint.2014.10.011

López-Barrera, F., Manson, RH., Landgrave, R., 2014. Identifying deforestation attractors and patterns of fragmentation for seasonally dry tropical forest in central Veracruz, Mexico. Land Use Policy. 41, 274-283. https://doi.org/10.1016/j.landusepol.2014.06.004

Luo, M., Liu, T., Meng, F., Duan, Y., Bao A., Frankl A., et al., 2019. Spatiotemporal characteristics of future changes in precipitation and temperature in Central Asia. Int. J. Climatol. 39, 1571-1588. https://doi.org/10.1002/joc.5901

Luo, Q., Zhou, J., Li, Z., Yu, B., 2020. Spatial differences of ecosystem services and their driving factors: A comparation analysis among three urban agglomerations in China's Yangtze River Economic Belt. Sci. Total Environ. 725, 138452.

https://doi.org/10.1016/j.scitotenv.2020.138452

Markevych, I., Schoierer, J., Hartig, T., Chudnovsky, A., Hystad, P., Dzhambov, AM., et al., 2017. Exploring pathways linking greenspace to health: Theoretical and methodological guidance. Environ. Res. 158, 301-317. https://doi.org/10.1016/j.envres.2017.06.028

Meyfroidt, P., Roy, Chowdhury R., de Bremond, A., Ellis, EC., Erb, KH., Filatova, T., et al., 2018. Middle-range theories of land system change. Glob. Environ. Change-Human Policy Dimens. 53, 52-67. https://doi.org/10.1016/j.gloenvcha.2018.08.006

Midekisa, A., Holl, F., Savory, D.J., Andrade-Pacheco, R., Gething, P.W., Bennett, A., et al., 2017. Mapping land cover change over continental Africa using Landsat and Google Earth Engine cloud computing. PLOS ONE 12(9), e0184926. https://doi.org/ 10.1371/journal.pone.0184926

Newman, ME., McLaren, KP., Wilson, BS., 2014. Long-term socio-economic and spatial pattern drivers of land cover change in a Caribbean tropical moist forest, the Cockpit Country, Jamaica. Agric Ecosyst Environ. 186, 185-200. https://doi.org/10.1016/j.agee.2014.01.030

Ou, C., Yang, J., Du, Z., Liu, Y., Feng, Q., Zhu, D., 2019. Long-Term Mapping of a Greenhouse in a Typical Protected Agricultural Region Using Landsat Imagery and the Google Earth Engine. Remote Sens. 12, 55. https://doi.org/10.3390/rs12010055

Peng, J., Zhao, M., Guo, X., Pan, Y., Liu, Y., 2017. Spatial-temporal dynamics and associated driving forces of urban ecological land: A case study in Shenzhen City, China. Habitat Int. 60, 81-90. https://doi.org/10.1016/j.habitatint.2016.12.005

Piao, S., Fang, J., Zhou, L., Guo, Q., Henderson, M., Ji, W., et al., 2003. Interannual variations of monthly and seasonal normalized difference vegetation index (NDVI) in China from 1982 to 1999. J. Geophys. Res.-Atmos. 108. https://doi.org/108. 10.1029/2002JD002848

Qiu, L., Pan Y., Zhu, J., Amable, GS., Xu, B., 2019. Integrated analysis of urbanization-triggered land use change trajectory and implications for ecological land management: A case study in Fuyang, China. Sci. Total Environ. 660, 209-217. https://doi.org/10.1016/j.scitotenv.2018.12.320

Scolozzi, R., Geneletti, D., 2012. A multi-scale qualitative approach to assess the impact of urbanization on natural habitats and their connectivity. Environ. Impact Assess. Rev. 36, 9-22. https://doi.org/10.1016/j.eiar.2012.03.001

Serret, H., Raymond, R., Foltête, J-C., Clergeau, P., Simon, L., Machon, N., 2014. Potential contributions of green spaces at business sites to the ecological network in an urban agglomeration: The case of the Ile-de-France region, France. Landsc. Urban Plan. 131, 27-35. https://doi.org/10.1016/j.landurbplan.2014.07.003

Seto, KC., Reenberg, A., Boone, CG., Fragkias, M., Haase, D., Langanke, T., et al., 2012. Urban land teleconnections and sustainability. Proc. Natl. Acad. Sci. U. S. A. 109, 7687. https://doi.org/10.1073/pnas.1117622109

Smith, P., Adams, J., Beerling, DJ., Beringer, T., Calvin, KV., Fuss, S., et al., 2019. Land-Management Options for Greenhouse Gas Removal and Their Impacts on Ecosystem Services and the Sustainable Development Goals. Annu. Rev. Environ. Resour. 44, 255-286. https://doi.org/10.1146/annurev-environ-101718-033129

Soltanifard, H., Jafari, E., 2019. A conceptual framework to assess ecological quality of urban green space: a case study in Mashhad city, Iran. Environ. Dev. Sustain. 21, 1781-1808.

https://doi.org/10.1007/s10668-018-0103-5

Sun, X., Lu, Z., Li, F., Crittenden, J.C., 2018. Analyzing spatio-temporal changes and trade-offs to support the supply of multiple ecosystem services in Beijing, China. Ecol. Indic. 94, 117-129. https://doi.org/10.1016/j.ecolind.2018.06.049

Thapa, BR., Murayama, Y., 2009. Examining Spatiotemporal Urbanization Patterns in Kathmandu Valley, Nepal: Remote Sensing and Spatial Metrics Approaches. Remote Sens. 1. https://doi.org/10.3390/rs1030534

The People's Government of Guangdong Provence., 2013. Decision on Comprehensively Promoting a New Round of Action to Green Guangdong. http://www.zhfjyl.com/ZtuDetail.aspx?MsgId=29 (accessed 28 July 2020).

Tilman, D., Cassman, KG., Matson, PA., Naylo,r R., Polasky, S., 2002. Agricultural sustainability and intensive production practices. Nature. 418, 671-677. https://doi.org/10.1038/nature01014

Wang, F., Wang, K., Liu, H., 2020. Evaluation and influence factors of spatial accessibility of ecological space recreation service in the Pearl River Delta Urban Agglomeration: a modified Two-step Floating Catchment Area method. Acta Ecologica Sinica. 40, 3622-3633 (in Chinese). https://doi.org/10.5846/stxb201901060046

Wang, J-F., Li, X-H., Christakos, G., Liao, Y-L., Zhang, T., Gu, X., et al., 2010. Geographical Detectors-Based Health Risk Assessment and its Application in the Neural Tube Defects Study of the Heshun Region, China. Int. J. Geogr. Inf. Sci. 24, 107-127. http://dx.doi.org/10.1080/13658810802443457

Wang, J-F., Zhang, T-L., Fu, B-J., 2016. A measure of spatial stratified heterogeneity. Ecol. Indic. 67, 250-256. https://doi.org/10.1016/j.ecolind.2016.02.052

Wang, J., He, T., Lin, Y., 2018. Changes in ecological, agricultural, and urban land space in 1984–2012 in China: Land policies and regional social-economical drivers. Habitat Int. 71, 1-13. https://doi.org/10.1016/j.habitatint.2017.10.010

Wang, Y., Wu, T., Li, H., Skitmore, M., Su, B., 2020. A statistics-based method to quantify residential energy consumption and stock at the city level in China: The case of the Guangdong-Hong Kong-Macao Greater Bay Area cities. J. Clean Prod. 251, 119637. https://doi.org/10.1016/j.jclepro.2019.119637

Wong, K., Zhang, Y., Tsou, YJ., Li, Y., 2017. Assessing Impervious Surface Changes in Sustainable Coastal Land Use: A Case Study in Hong Kong. Sustainability. 9, 1029. https://doi.org/10.3390/su9061029

Xie, H., He, Y., Xie, X., 2017. Exploring the factors influencing ecological land change for China's Beijing–Tianjin–Hebei Region using big data. J. Clean Prod. 142, 677-687. https://doi.org/10.1016/j.jclepro.2016.03.064

Xie, H., Liu, Z., Wang, P., Liu, G., Lu, F., 2014. Exploring the Mechanisms of Ecological Land Change Based on the Spatial Autoregressive Model: A Case Study of the Poyang Lake Eco-Economic Zone, China. INT J ENV RES PUB HE. 11, 583-599. https://doi.org/10.3390/ijerph110100583

Xu, Z., Zhang, Z., Li, C., 2019. Exploring urban green spaces in China: Spatial patterns, driving factors and policy implications. Land Use Policy. 89, 104249. https://doi.org/10.1016/j.landusepol.2019.104249

Yang, C., Li, Q., Zhao, T., Liu, H., Gao, W., Shi, T., ea al., 2019. Detecting Spatiotemporal

Features and Rationalities of Urban Expansions within the Guangdong–Hong Kong–Macau Greater Bay Area of China from 1987 to 2017 Using Time-Series Landsat Images and Socioeconomic Data. Remote Sens. 11, 19. https://doi.org/10.3390/rs11192215

Yang, J., Zeng, C., Cheng, Y., 2020. Spatial influence of ecological networks on land use intensity. Sci. Total Environ. 717, 137151. https://doi.org/10.1016/j.scitotenv.2020.137151

Zhang, G., Biradar, C., Xiao, X., Dong, J., Zhou, Y., Qin, Y., et al., 2017. Exacerbated grassland degradation and desertification in Central Asia during 2000□2014. Ecol. Appl. 28, 442-456. https://doi.org/10.1002/eap.1660

Zhang, L., Jin, G., Wan, Q., Liu, Y., Wei, X., 2018. Measurement of Ecological Land Use/Cover Change and Its Varying Spatiotemporal Driving Forces by Statistical and Survival Analysis: A Case Study of Yingkou City, China. Sustainability. 10, 4567. https://doi.org/10.3390/su10124567

Zhang, Y., Hu, Y., Zhuang, D., 2020. A highly integrated, expansible, and comprehensive analytical framework for urban ecological land: A case study in Guangzhou, China. J. Clean Prod. 268, 122360. https://doi.org/10.1016/j.jclepro.2020.122360

Zhao, Y., Gong, P., Yu, L., Hu, L., Li, X., Li, C., et al., 2014., Towards a common validation sample set for global land-cover mapping. Int. J. Remote Sens. 35, 4795-4814. https://doi.org/10.1080/01431161.2014.930202

Zhou, W., Mu, R., 2019. Exploring Coordinative Mechanisms for Environmental Governance in Guangdong-Hong Kong-Macao Greater Bay Area: An Ecology of Games Framework. Sustainability. 11, 3119. https://doi.org/10.3390/su11113119

Zhu, Z., Wang, S., Woodcock, C., 2015. Improvement and expansion of the Fmask algorithm: Cloud, cloud shadow, and snow detection for Landsats 4-7, 8, and Sentinel 2 images. Remote Sens. Environ. 159, 269-277. https://doi.org/10.1016/j.rse.2014.12.014

Appendix A

In this work, we employed the Modified Normalized Difference Water Index (MNDWI) for enhancing the contrast between water and others (McFeeters, 1996), Soil Adjusted Vegetation Index (SAVI) for eliminating soil background noise from vegetation (Huete, 1988), Normalized Difference Built-Up Index (NDBI) for extracting built-up areas (Zha et al., 2003)and Normalized Difference Vegetation Index (NDVI) for enhancing the vegetation and no-vegetation (Kindu et al., 2013). These variables can be calculated using Eqs. (A1-A4) from the Landsat image bands.

MNDWI, SAVI, NDBI and NDVI can be expressed as follows:

$$MNDWI = (B_{Green} - B_{SWIR})/(B_{Green} + B_{SWIR}) \quad \text{(A1)}$$

$$SAVI = (B_{NIR} - B_{Red})\,(1 + L)/(B_{NIR} - B_{Red} + L) \quad \text{(A2)}$$

$$NDBI = (B_{SWIR} - B_{NIR})/(B_{SWIR} + B_{NIR}) \quad \text{(A3)}$$

$$NDVI = (B_{NIR} - B_{Red})/(B_{NIR} - B_{Red}) \quad \text{(A4)}$$

where Green, SWIR, NIR and Red represent reflectance of TM Bands 2, 5, 4 and 3, respectively, L is a soil adjustment factor, and 0.5 was usually chosen to remove soil background (Huete, 1988).

Tab. A1 Policies of ecological land in the Guangdong-Hong Kong-Macao Greater Bay Area

Year	Policy	Main content
2001	Ecological Environment Construction Planning in Guangdong Province	Implementing projects to build protective forest systems and urban forestry; Building ecotourism sites that combine natural landscapes with excellent ecological environments.
2009	Outline Development Plan for the Pearl River Delta (2008-2020)	Promoting the construction of urban landscape forests, urban public green spaces and green belts around cities; Accelerating the completion of green belts along highways and railways to form networked regional ecological corridors.
2013	A New Round of Greening Guangdong	Investing in key forestry ecological projects, transforming the mode of ecological forestry development and improving the forest ecological compensation mechanism
2014	Integrated Plan for Ecological Security System in the Pearl River Delta (2014-2020)	Strengthening the sealing of mountains and forestation, strictly control the size of the population and development activities; Controlling the total amount of construction land, and strictly limiting the conversion of ecological land into construction land.
2014	Guangdong Province Ecological Protection Compensation Measures	Increasing investment in ecological protection, providing appropriate compensation to cities in key ecological function zones through transfer payments to enhance basic public service sand coordination between economic development and the ecological environment.
2017	Pearl River Delta National Forest Urban Agglomeration Construction Plan (2016-2025)	Implementing ten key ecological projects, including the construction of national forest cities, forest towns, green ecological water networks, regional ecological corridors, forests into urban enclosures, forest recreation bases, coastal protection forests, nature education bases and smart forest cities, and the precise improvement of forest quality.
2019	Outline Development Plan for the Guangdong-Hong Kong-Macao Greater Bay Area	Implementing major projects for the protection and restoration of important ecosystems, building an ecological corridor and biodiversity protection network, and improving the quality and stability of ecosystems; Defining and strictly observing the ecological protection red line, strengthening the control of natural ecological space.

Tab. A2 Datasets used in this research

	Data	Data Sources	Spatial Resolution	Time series
Datasets	Landsat	http://landsat.usgs.gov	30m	1990-2019
	Land use remote sensing monitoring dataset	http://www.resdc.cn	1 km	2000-2015
Driving factors	Elevation	http://www.resdc.cn/data.aspx?DATAID=217	30m	-
	Slope	Calculated according to elevation	30m	-
	Average annual precipitation	https://data.nodc.noaa.gov/cgi-bin/	0.25 arc degrees	1990-2019
	Average annual temperature	http://www.climatologylab.org/terraclimate.html	2.5 arc minutes	1990-2019
	Resident population density	http://www.stats.gov.cn/tjsj/	-	1990-2019
	Land urbanization rate	Calculated according to the land cover data in this article	-	1990-2019
	Population and GDP per capita	http://www.stats.gov.cn/tjsj/	-	1990-2019

Tab. A3 Landscape metrics used in this study

Metric	Abbreviation	Description	Equation
Patch density	PD	Number of greenspace patches divided by the total landscape area	n/km^2
Edge density	ED	Total length of all edge segments in the greenspace per hectare	m/ha
Contagion index	CONTAG	The extent of the dispersion of different land cover types in the landscape.	%
Shannon's diversity index	SHDI	A measure of the diversity of patch types in a landscape that is determined by both the number of different patch types and the proportional distribution of area among patch types.	Information

Tab. A4 The areas and proportions of ecological land in each region of Guangdong-Hong Kong-Macao Greater Bay Area in 1990, 2000, 2005, 2010 and 2019

	1990		2000		2010		2019	
	Area (km^2)	Proportion(%)	Area (km^2)	Proportion(%)	Area (km^2)	Proportion(%)	Area (km^2)	Proportion(%)
Overall	26716.14	47.19	26231.04	46.34	25331.58	44.75	25346.79	44.77
ZQ	9838.44	64.04	9835.38	64.02	9511.83	61.91	9512.55	61.92
HZ	5722.74	49.20	5637.33	48.47	5608.44	48.22	5687.28	48.90
JM	3298.59	34.81	3214.44	33.92	3186.18	33.63	3238.56	34.18
GZ	2952.18	39.96	2880.99	38.99	2854.26	38.63	2928.87	39.64
FS	1367.1	35.05	1291.32	33.10	1143.36	29.31	1049.04	26.89
DG	828.18	32.94	737.37	29.33	578.16	23.00	548.28	21.81
ZH	711.9	47.05	689.13	45.54	659.25	43.57	641.97	42.43
SZ	709.47	36.66	653.85	33.79	548.37	28.34	542.88	28.05
ZS	682.47	38.77	639.18	36.31	583.65	33.15	531.09	30.17
HK	593.55	53.77	644.4	58.38	652.14	59.08	661.14	59.89
MC	11.52	44.44	7.65	29.51	5.94	22.92	5.13	19.79

Tab. A5 Transfer matrix between ecological land and non-ecological in Guangdong-Hong Kong-Macao Greater Bay Area (km^2)

		Ecological land			Non-Ecological land		Total
		Forestland	Grassland	Water bodies	Construction land	Other land	
1990-2000							
Ecological land	Forestland	21640.77	0.18	4.13	20.52	542.98	22208.58
	Grassland	37.26	1010.25	4.68	272.52	88.74	1413.45
	Water bodies	19.89	5.58	3000.42	13.50	54.72	3094.11
Non-Ecological land	Construction land	0	0	0	2104.11	0	2104.11
	Other land	492.29	0.08	15.48	537.31	26745.93	27791.09
2000-2010							
Ecological land	Forestland	21540.6	0.82	2.88	62.82	583.11	22190.23
	Grassland	2.88	388.71	1.08	616.41	7.02	1016.1
	Water bodies	68.49	26.46	2825.64	82.08	22.05	3024.72
Non-Ecological land	Construction land	0	0	0	2947.95	0	2947.95
	Other land	313.91	0.36	3.24	2803.86	24310.97	27432.34
2010-2019							
Ecological land	Forestland	21796.58	0	0.55	39.34	154.24	21990.71
	Grassland	0.36	286.39	0	185.74	0	472.5
	Water bodies	9.00	0.56	2833.22	25.33	0.28	2868.39
Non-Ecological land	Construction land	43.67	35.60	153.06	5909.63	27.24	6016.14
	Other land	425.94	0	0.99	1150.66	23686.04	25263.63

References

Huete, A., 1988. A Soil-Adjusted Vegetation Index (SAVI). Remote Sens. Environ. 25, 295-309. https://doi.org/10.1016/0034-4257(88)90106-x

Kindu, M., Schneider, T., Teketay, D., Knoke, T., 2013. Land Use/Land Cover Change Analysis Using Object-Based Classification Approach in Munessa-Shashemene Landscape of the Ethiopian Highlands. Remote Sens. 5, 2411-2435. https://doi.org/10.3390/rs5052411

McFeeters, S., 1996. The Use of Normalized Difference Water Index (NDWI) in the Delineation of Open Water Features. Int. J. Remote Sens. 17, 1425-1432. https://doi.org/10.1080/01431169608948714

Zha, Y., Gao, J., Ni, S., 2003. Use of normalized difference built-up index in automatically mapping urban areas from TM imagery. Int. J. Remote Sens. 24, 583-594. https://doi.org/10.1080/01431160304987

Highlights

- Quantifying the interaction and evolution of driving factors on ecological land
- Population density determines the majority area of the ecological land evolution
- Socioeconomic factors were more influential than natural factors on ecological land
- The interaction between population density and elevation had the largest influence
- The impact of temperature and precipitation declined by 69% and 77%, respectively

Declaration of interests

☒ The authors declare that they have no known competing financial interests or personal relationships that could have appeared to influence the work reported in this paper.

☐The authors declare the following financial interests/personal relationships which may be considered as potential competing interests: